Toward *p*-Octiphenyl β-Barrel RNases

Bodo Baumeister and Stefan Matile*

Department of Organic Chemistry, University of Geneva, CH-1211 Geneva 4, Switzerland

Received September 10, 2001; Revised Manuscript Received December 3, 2001

ABSTRACT: A synthetic barrel-stave supramolecule with *p*-oligophenyl "staves" and β-sheet "hoops" is shown to catalyze the hydrolysis of a doubly labeled homooligomeric model RNA 32 000 times compared to imidazole in water at nanomolar concentrations, 50 °C, and pH 7.0. RNase activity of this rigid-rod β-barrel is shown to depend on pH (maximal at pH 5.5) and Zn^{2+} (up to 7-fold increase). Denaturation kinetics suggest that an intact suprastructure is essential for activity and that RNA and Zn^{2+} exhibit a stabilizing template effect. Product analysis by HPLC is indicative for selective RNase activity with respect to substrate length.

Introduction

The design of artificial ribonucleases (RNases) has received much scientific attention because of the medicinal perspective of controlled inhibition of gene expression by selective cleavage of mRNA.[1−5] Most artificial RNases with substantial activity known today take advantage of modern bioinorganic chemistry.[1−3] Nevertheless, a rich variety of metal-free catalysts have been created over the past two decades, combining many bifunctional alkylamines, imidazoles, guanidinium cations, and mixed dimers with divers recognition motifs.[1−15]

Intense research on imidazole-rich artificial RNases was stimulated by the fact that pancreatic bovine ribonuclease A (RNase A) acts by general acid/base catalysis using two neighboring histidine residues.[1,4−6] Combination of the intrinsic catalytic activity of imidazole dyads with selective binding has been investigated in conjugates of cyclodextrins,[8] *N*-phenazinium[9] and acridine[13,14] intercalators, dicationic 1,4-diazabicyclo-[2.2.2]octane[10] and tetracationic spermines,[11] minor-groove selective lexitropsins,[12] and antisense oligonucleotides.[15,16] In part, high selectivities were reported together with characteristic activities reaching from 10% to 100% RNA cleavage in 4−18 h at temperatures between 37 and 50 °C and catalyst concentrations of 50 μM−2.5 mM.[8−16]

Results from a different line of research have indicated high importance of β-sheet secondary and perhaps tertiary structures for RNase activity.[7] Barbier and Brack demonstrated that the activity of poly(LK) and, to a smaller extent, that of poly(LR) exceeds that of the "non-β" poly(K), poly(H), poly(AK), poly(PLKLK), "racemized" poly(LK), and monomeric LK-dipeptides (K: L-lysine, R: L-arginine, L: L-leucine, A: L-alanine). The highest activity identified for poly(LK) (i.e., cleavage of 400 μM RNA in 1 week at 37 °C and pH = 7.5 by 1 mM catalyst, 185 times beyond autohydrolysis) was rationalized to originate from topological matching of the charges on poly(LK)-β-sheets and RNA. The for this report highly relevant poly(LH) was not studied because of insolubility in water.[7]

Extensive information was thus on hand to identify a histidine- *and* β-sheet-rich barrel-stave supramolecule such as **1** as potential RNase (Figure 1). *p*-Octiphenyl β-barrel **1** is a novel rigid-rod β-barrel[17,18] composed of four preorganizing rigid-rod staves[19,20] and 32 interdigitating pentapeptide β-strands of the sequence L-leucine-L-histidine-L-leucine-L-histidine-L-leucine (LHLHL) that position 64 histidine residues along a central

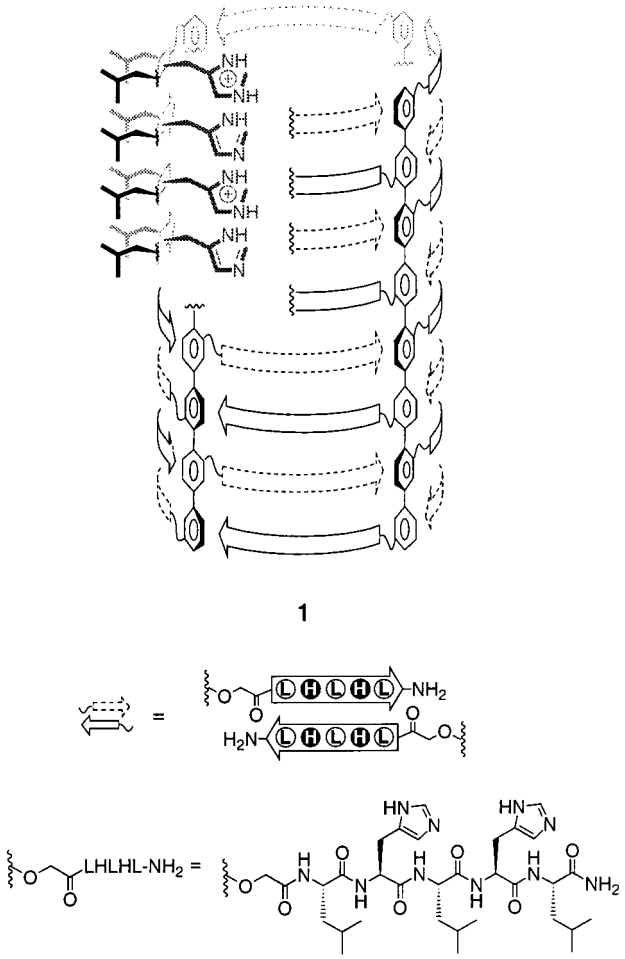

Figure 1. Putative cutaway suprastructure of catalytic rigid-rod β-barrel **1**. β-Strands are depicted as arrows pointing to the C-terminus, amino acid residues (one-letter abbreviation) pointing toward the exterior are black on white, internal residues white on black; β-strand topology is further visualized in the cutaway on the upper left. (Concentrations refer to tetrameric supramolecules throughout the text if not otherwise indicated, and the depicted 50% histidine protonation is chosen arbitrarily.)

* Corresponding author. e-mail: stefan.matile@chiorg.unige.ch.

10.1021/ma011612m CCC: $22.00
Published on Web 01/29/2002

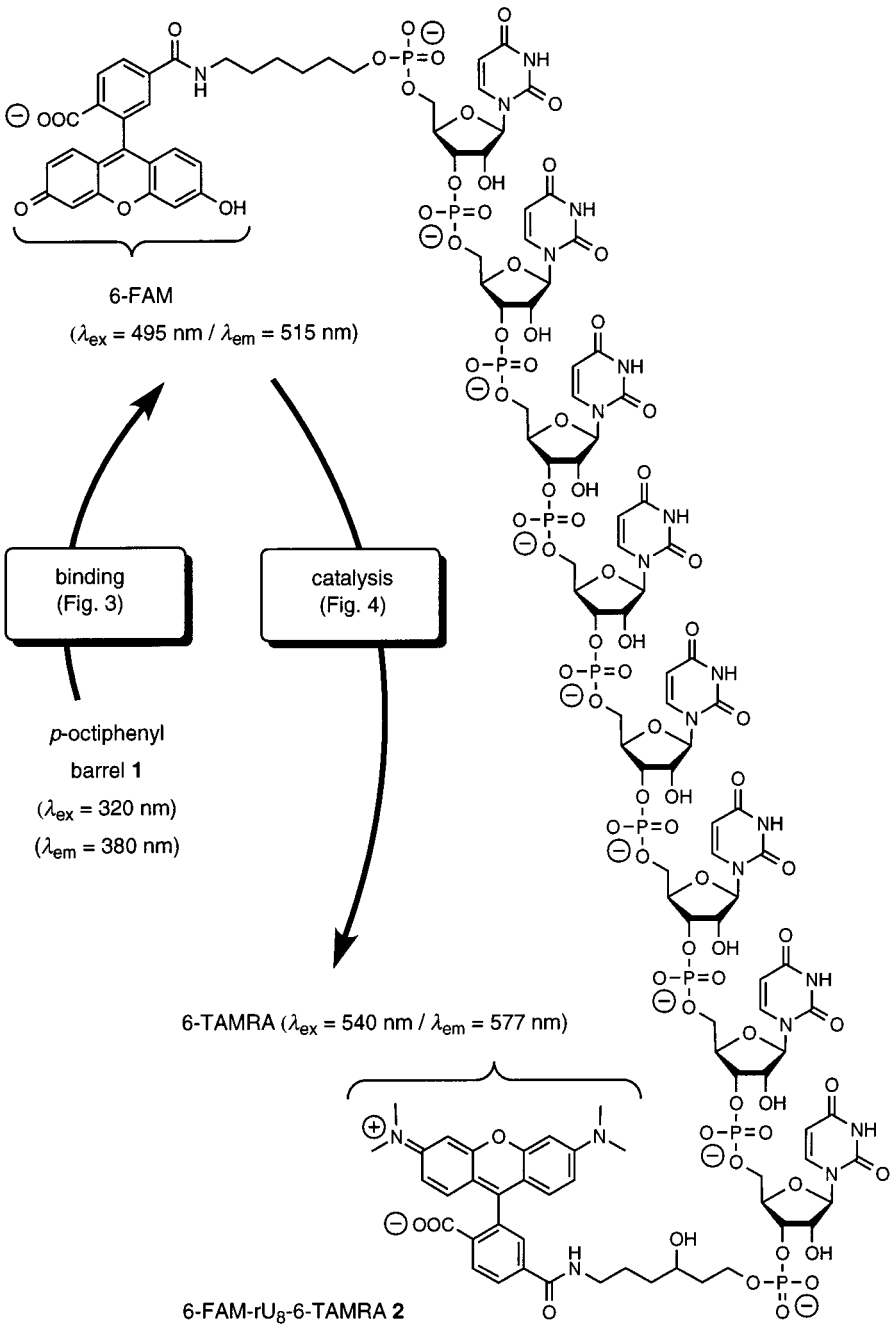

Figure 2. Structure of doubly labeled oligoribonucleotide substrate 6-FAM-rU$_8$-6-TAMRA **2** with indication of the possibility to detect substrate binding and hydrolysis by fluorescence resonance energy transfer (FRET) from the *p*-oligophenyl donors (using λ_{ex} = 320 nm) and the fluorescein donor/acceptor (using λ_{ex} = 495 nm), respectively, to the rhodamine acceptor.

hydrophilic channel.[21] Insights from atomic force microscopy,[21a] single and multichannel conductance experiments in planar bilayer membranes,[21b] dye leakage experiments in spherical bilayer membranes,[21c] and esterolysis of organic trianions in isotropic and anisotropic media[21b] indicate that tetramer **1** with ion channel, guest binding, and esterolytic activity[21b] forms in water as well as in bilayer membranes at monomer concentrations $\leq 3\ \mu$M. The fibrillogenic activity of rigid-rod β-barrel **1** above 3 μM limits functional studies to nanomolar and hampers conventional structural studies at elevated concentrations.[21a] Although the precise barrel stoichiometry could so far not be verified experimentally, we decided to use a tetramer (i.e., **1**) as a working model with the only intention to simplify calculations and text. This assumption is, however, strongly supported by molecular models,[17a,f] previous results,[17] and the magnitude of the single channel conductance.[21b]

In the following, we report that *p*-octiphenyl β-barrels **1** (Figure 1) accelerate buffer catalyzed hydrolysis of the doubly labeled oligoribonucleotide model substrate 6-FAM-rU$_8$-6-TAMRA **2** (Figure 2) 32 000 times compared to imidazole in water at nanomolar concentrations, 50 °C, and pH 7.0. We further describe the pH and denaturation profile of, the influence of Zn^{2+} on, and the product distribution obtained with this novel, histidine- and β-sheet-rich artificial RNase.

Materials and Methods

General. The synthesis and characterization of barrel **1** are reported elsewhere.[21b] RP-HPLC purification of barrel **1** prior

to use was performed routinely under denaturating conditions (YMC-ODS A, MeOH: H_2O: TFA, 79.5:19.5:1, 3 mL/min, R_t = 7.51 min). Concentrations of dilute samples were confirmed by UV−vis spectroscopy assuming ϵ(*p*-octiphenyl) = 28.6 mM^{-1} cm^{-1} (320 nm)[17] and refer to tetrameric self-assemblies (i.e., β-barrel **1**) if not otherwise indicated. Synthetic 6-FAM-rU_8-6-TAMRA **2** of >98% purity (HPLC) was obtained from Microsynth GmbH (Balgach, Switzerland). Concentrations of dilute samples were confirmed by UV−vis spectroscopy. RNase A, imidazole, detergents, all salts, and buffers were of the best grade available from Sigma and used as received. UV−vis spectra were recorded on a Varian Cary 1 Bio spectrophotometer equipped with a stirrer and a temperature controller. CD spectra were recorded on a JASCO-710 spectropolarimeter. HPLC measurements were done using YMC-ODS A reverse phase or NUCLEOGEN DEAE 60-7 ion-exchange columns (Macherey-Nagel, Germany), a Jasco PU-980 pump, and a Jasco UV-970 UV−vis/fluorescence detector. Fluorescence spectra were recorded on FluoroMax-2 (Jobin Yvon-Spex) equipped with an injector port, a stirrer, and a temperature controller. Abbreviations: 6-FAM = 5′,6-carboxyfluorescein; FRET = fluorescence resonance energy transfer; GuHCl = guanidinium chloride; HEPES = 4-(2-hydroxyethyl)piperazine-1-ethanesulfonic acid; 6-TAMRA = 3′,6-carboxytetramethylrhodamine. Standard abbreviations are used for peptides and oligonucleotides.

RNA Binding, FRET Assay. A solution of β-barrel **1** (0−500 nM) and 6-FAM-rU_8-6-TAMRA **2** (0−200 nM) in 50 mM HEPES at pH 7.0 was incubated for 10 min at 50 °C. An aliquot of 50 μL was added to a stirred cuvette containing 1950 μL of buffer (50 mM HEPES, pH 7.0, 20 °C). The emission spectrum of this solution was recorded upon excitation at 320 nm; slits were adjusted appropriately. A control sample without barrel **1** was treated the same way.

RNA Hydrolysis, FRET Assay.[22] To a solution of 6-FAM-rU_8-6-TAMRA **2** (25−200 nM) in 50 mM HEPES, pH 5−8, 20 μL of concentrated stock solutions of β-barrel **1** (0−500 nM), imidazole (0−10 mM), $ZnCl_2$ (0−4 μM), GuHCl (0−2 M), and KCl (0−2 M) were added to give the indicated concentrations. The reactions were performed at 50 °C in the dark. At given time intervals, aliquots of 200 μL were taken and diluted to 2 mL with 2 M $NaClO_4$, 50 mM HEPES using pH 7.3 to secure maximal emission intensities. Emission spectra were recorded upon excitation at 495 nm; slits were adjusted appropriately and then kept constant. The ratio $(I_{515}/I_{577})_t$ of emission intensity at 515 nm (for fluorescein) and 577 nm (for rhodamine) was then determined. The total concentration of 6-FAM-rU_{0-8} products was calculated from $(I_{515}/I_{577})_t$ by calibration with $(I_{515}/I_{577})_{t(0)}$ and $(I_{515}/I_{577})_{t(\infty)}$. $(I_{515}/I_{577})_{t(0)}$ was determined experimentally prior of each experiment using the same procedure; $(I_{515}/I_{577})_{t(\infty)}$ was determined after each experiment by addition of an excess of RNase A. Plots of the concentration of 6-FAM-rU_{0-8} products as a function of time were then used to calculate the apparent pseudo-first-order rate constants k. For pH and denaturation profiles, relative rates were calculated by dividing individual rate constants k by the highest observed rate constant k_{max}. Denaturation profiles were further analyzed following the procedure described by Ahmad and Bigelow without change.[23] Elimination of the isolate contribution of ionic interactions to denaturation curves using KCl instead of GuHCl gave qualitatively correct results, but quantitative evaluation failed because of precipitation after addition of KCl solutions to 2 M $NaClO_4$, 50 mM HEPES, pH 7.3.

RNA Hydrolysis, HPLC Assay. Aliquots of 100 μM were taken from RNA hydrolysis under above conditions and injected. Product separation was possible with ion-exchange NUCLEOGEN DEAE 60-7 columns as stationary, a linear gradient from 100% 20 mM KH_2PO_4, pH 5.5 to 100% 1 M KCl, 20 mM KH_2PO_4, pH 5.5 in 1 h as mobile phase,[24] and a flow rate of 1 mL/min. 6-FAM-rU_{0-8} products were detected selectively with λ_{ex} 495 nm and λ_{em} 515 nm.

CD Spectroscopy. Spectra for **1** were measured in 50 mM HEPES at the indicated pH, 20 °C. $\Delta\epsilon$ values refer to monomeric *p*-octiphenyl concentrations. CD denaturation plots were obtained by titration with GuHCl and analyzing the observed decrease of all CD Cotton effects. The $\Delta\epsilon_{max}$ at 317 nm at indicated GuHCl concentrations c ($\Delta\epsilon_c$) was used to calculate the fraction of denatured barrel $f_D = (\Delta\epsilon_N - \Delta\epsilon_c)/(\Delta\epsilon_N - \Delta\epsilon_D)$; $\Delta\epsilon_N = -10.0$ M^{-1} cm^{-1} (Figure 7, solid); $\Delta\epsilon_D = -2.0$ M^{-1} cm^{-1}. K_D and ΔG^{H2O} were not determined[23] because $C_{50} \leq 0.3$ M GuHCl.

Results and Discussion

RNA Design. Doubly labeled uridine homooligomer **2** was selected as model substrate (Figure 2).[22] Judged from their Förster radius of R_0 = 55 Å,[25] it was conceivable that the 5′,6-carboxyfluorescein (6-FAM) donor and the 3′,6-carboxytetramethylrhodamine (6-TAMRA) acceptor are positioned close enough in intact substrate **2** for full quenching of emission of 6-FAM by fluorescence resonance energy transfer (FRET). Removal of the acceptor 6-TAMRA during ribonucleotide hydrolysis would then allow the detection of the gradual increase in overall concentration of "6-TAMRA-free" 5′-RNA fragments 6-FAM-rU_{0-8} by the increase in donor emission as a function of time. An up to 180-fold increase in 6-FAM emission reported recently for optimized doubly labeled tetranucleotide substrates demonstrated that this FRET-based assay is the most sensitive RNase assay known today and that the two terminal labels do not influence the kinetics of RNase A.[22]

The use of this "hypersensitive" RNase assay in this study was crucial. It was particularly important to realize that less sensitive methods would not be compatible with the present system, because β-barrel **1** is known to transform into β-fibrils at monomer concentrations above 3 μM.[21a] Moreover, it was expected that the *p*-oligophenyl fluorophores in the barrel catalyst **1** could serve as additional donors[26] to report substrate binding by FRET to the rhodamine acceptor in the substrate, either directly or mediated through the fluorescein fluorophore with intermediate energy.

Because of the poorly ordered structure of its single-stranded oligomers,[27] uridine was the nucleoside of choice to study hydrolysis with minimized influences from substrate self-organization. The length of homooligomeric substrate **2** was adjusted to that of homooligomeric catalyst **1**.[17c,28]

RNA Binding. The appearance of rhodamine emission at 577 nm upon excitation of the *p*-octiphenyl donors at 320 nm confirmed binding of 6-FAM-rU_8-6-TAMRA **2** to *p*-octiphenyl β-barrel **1** at the relevant nanomolar concentrations (Figure 3, solid line). As discussed above, fluorescence resonance energy transfer (FRET) from host **1** to guest **2** is only possible if the host-donor and guest-acceptor fluorophore are in close proximity in space, i.e., form a host−guest complex. Control experiments without *p*-octiphenyl donors **1** did not exhibit similar rhodamine emission under identical conditions (Figure 3, dotted line).

As expected from many reports on binding of oligonucleotides to polycationic hosts, precipitation of presumably higher-order complexes was observed, particularly at micromolar concentrations. In support of the central importance of electrostatic interactions between host and guest, these heterooligomeric precipitates could, however, be redissolved with 2 M $NaClO_4$. The latter behavior was reported previously for lysine- and arginine-rich polypeptide RNases.[7]

RNA Hydrolysis. Whereas FRET from the high-energy *p*-octiphenyl donors in the barrel host thus turned out to be useful to monitor binding of RNA guests

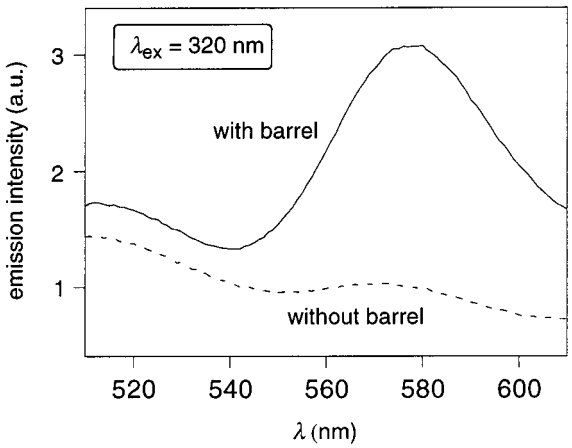

Figure 3. Representative emission spectra ($\lambda_{ex} = 320$ nm) for 6-FAM-rU$_8$-6-TAMRA **2** (50 nM, 50 mM HEPES, pH 7.0, 50 °C) in the presence (solid) and absence (dashed) of *p*-octiphenyl β-barrel **1** (125 nM), measured at 20 °C after dilution (see Methods section).

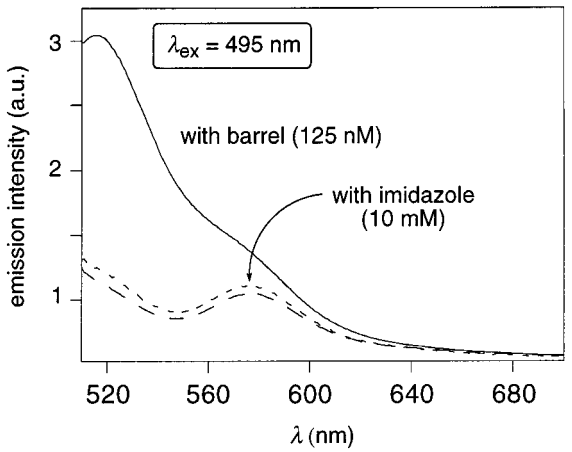

Figure 4. Representative emission spectra ($\lambda_{ex} = 495$ nm) for hydrolysis of 6-FAM-rU$_8$-6-TAMRA **2** (50 nM, 50 mM HEPES, pH 7.0, 50 °C) in the presence of 125 nM *p*-octiphenyl β-barrel **1** (dashed, solid) and 10 mM imidazole (dashed, dotted) at $t =$ 0 h (dashed) and $t = 23$ h (solid, dotted).

(Figure 3), changes in FRET from the low-energy 6-FAM donors to the 6-TAMRA acceptors at the other end of the substrate oligomer were ideal to follow RNA cleavage at nanomolar concentrations (Figure 4). Nearly quantitative FRET in intact 6-FAM-rU$_8$-6-TAMRA **2** was indicated by efficient quenching of the highly intense donor emission around 515 nm and substantial acceptor emission around 577 nm (Figure 4, dashed spectrum). The obtained spectrum was in agreement with the examples from the Raines group.[22] It remained nearly unchanged for days, also in the presence of up to 10 mM imidazole at 50 °C (Figure 4, dotted spectrum; Figure 5a, ○). The presence of 125 nM β-barrel **1**, however, caused rapid increase in donor emission during the first 4 h (Figure 4, solid spectrum; Figure 5a, ●). These observations were consistent with barrel-mediated separation of 6-FAM donors and 6-TAMRA acceptors in space, that is, barrel-catalyzed RNA hydrolysis.

Complete hydrolysis needed to calibrate the relative emission intensities was obtained by addition of an excess of RNase A at the end of each experiment. The increase in concentration of 6-FAM-rU$_{0-8}$ products as a function of time (Figure 5a, ●) calculated to a $k = 1.3 \times 10^{-4}$ min^{-1}. The rate of imidazole catalysis was not measurable under identical conditions (Figure 4). To

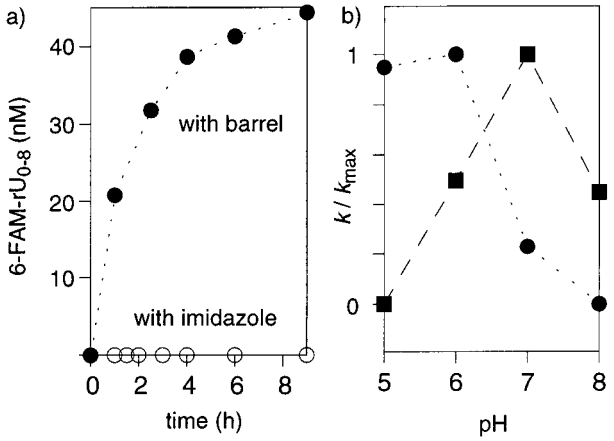

Figure 5. (a) Formation of 6-FAM-rU$_{0-8}$ from 6-FAM-rU$_8$-6-TAMRA **2** (50 nM) as a function of time in the presence 125 nM β-barrel **1** (●) and 10 mM imidazole (○, 50 mM HEPES, pH 7.0, 50 °C). (b) pH profile for the rate of hydrolysis of 6-FAM-rU$_8$-6-TAMRA **2** with 125 nM β-barrel **1** in absence (●) and presence (■) of 4 μM $ZnCl_2$ (50 mM HEPES, 50 °C).

estimate the rate enhancement of barrel compared to buffer catalysis for identical monomer concentration, the rate of buffer-catalyzed RNA hydrolysis was therefore determined at imidazole concentrations high enough to give reliable results and then extrapolated to the required concentrations (Figure 5a, ○). A 32 000-fold rate enhancement was found at pH = 7. Although different, often nontrivial experimental conditions and di- or oligomeric substrates and catalysts complicate meaningful interpretations, this activity of β-barrel RNase **1** compared qualitatively well with that reported for other imidazole-rich artificial RNases (see Introduction).[1−16] Note that the activity of β-barrel RNase **1** further increases under mildly acidic conditions and in the presence of Zn^{2+} (vide infra).

Effects of pH and Denaturants. The pH profile for RNase activity of β-barrel **1** revealed maximal activity under mildly acidic conditions (Figure 5b, ●). The identity of this maximal RNase activity around pH 5.5 with that of maximal esterase activity[21b] provided the first indication that self-assembly of a barrel-stave supramolecule (as in Figure 1) is required for efficient bifunctional acid/base catalysis. Further experimental support for the importance of such refined supramolecular architectonics came from denaturation experiments. Being aware of the usefulness of chaotropic agents to quantitatively assess peptide and protein self-organization,[17c,23] the catalytic activity of artificial RNase **1** was determined in the presence of increasing concentrations of guanidinium chloride as representative denaturant (Figure 6, ●). The observed sigmoidal decrease in activity with increasing denaturant concentration demonstrated that the effect of guanidinium chloride exceeds known contributions of ionic strength. The denaturation profile of RNase **1** thus implied importance of intact β-structure for function.

A routine extrapolation of denaturation curves as in Figure 6 (●) to the situation in denaturant-free water[23] gave a $\Delta G^{H_2O} = -1.2$ kcal/mol for the "active" complex formed between β-barrel **1** and RNA **2**. Please note that any interpretation of this value must not be done without appropriate reservation reflecting all not recognized effects that may further influence the outcome of denaturation kinetics.

A qualitative comparison of the "apparent" stability of the β-barrel/RNA complex with that of apo-β-barrel

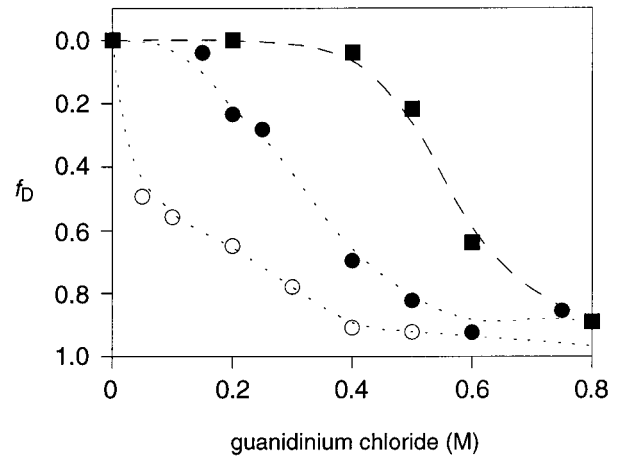

Figure 6. Dependence of the rate of hydrolysis of 50 nM 6-FAM-rU$_8$-6-TAMRA **2** by 125 nM β-barrel **1** in absence (●, $k_{max} = 1.3 \times 10^{-4}$ min^{-1}) and presence (■, $k_{max} = 9.1 \times 10^{-4}$ min^{-1}) of 4 μM $ZnCl_2$ on the concentration of guanidinium chloride (50 mM HEPES, 50 °C, pH 7.0) expressed as fraction of denatured barrel $f_D = 1 - (k/k_{max})$ for qualitative comparison with the CD denaturation curve of **1** (○). Lines are added to guide the eye only.

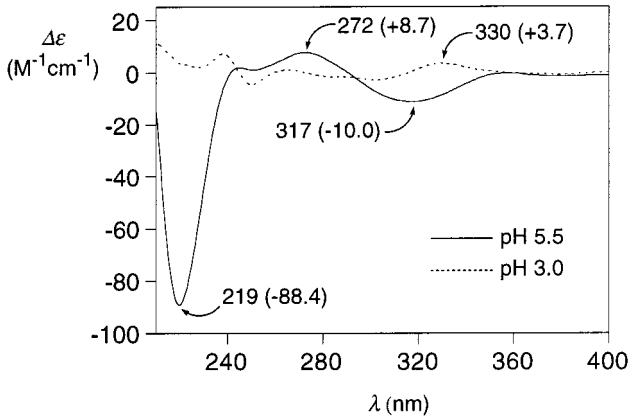

Figure 7. Representative CD spectra of intact and "deconstructed" rigid-rod β-barrel **1** in water at pH 5.5 and 3.0, respectively.

1 was made using circular dichroism (CD) spectroscopy (Figure 7). This method was of interest because it is sufficiently sensitive to study β-barrel **1** in absence (but not in the presence, vide supra) of RNA below the critical fibrillogenesis concentration.[21a] CD studies of *p*-oligophenyl β-barrels constructed by the better characterizable programmed assembly of complementary peptide rods[17f,g,c] (rather than self-assembly as with **1**) suggested that a first negative (here at 317 nm) followed by a second positive Cotton effect (here at 272 nm) is indicative for β-barrel suprastructures (Figure 7, solid). Interpretation of the unusually intense negative Cotton effect at 219 nm as proof of β-sheet conformation is appealing but not unproblematic because contributions of the chiral *p*-oligophenyl chromophore are expected in this region as well. The disappearance of the characteristic CD Cotton effects between pH 4 and 3 (Figure 7, dotted) was consistent with β-barrel deconstruction by internal charge repulsion between "overprotonated" histidines.

The magnitude of all characteristic CD Cotton effects decreased rapidly with increasing denaturant concentration (Figure 6, ○). This result was in agreement with the unprecedented[17c,e] lability of *p*-octiphenyl β-barrel **1** identified previously by single channel measurements.[21b] The "apparent" stability of the β-barrel/RNA complex was higher than that estimated for β-barrel **1** (Figure 6, ● vs ○). Although comparison of different denaturation experiments needs appropriate caution, this suggested that polyanionic substrate **2** exhibits a stabilizing "template" effect on supramolecular catalyst **1**. Influences of internal (carotenoid) "templates" on rigid-rod β-barrels (comprising internal leucines instead of histidines) have been observed previously.[17f]

Effects of Zinc Cations. The acceleration of RNA hydrolysis by $ZnCl_2$ in absence and particularly in the presence of imidazole buffer is well-known, and the mechanisms of catalysis are elucidated in detail.[1−16] It was thus not surprising to observe an maxiamal 7-fold increase in RNase activity of β-barrel **1** in the presence of $ZnCl_2$ (Zn^{2+}/histidine ≥ 1:2). The presence of $ZnCl_2$ further changed the pH profile for β-barrel RNase **1** in a manner that was in full agreement with extensive pertinent literature (Figure 5b, ■; note that the apparent decrease in activity above pH = 7 is known to originate from precipitation of zinc hydroxide[1−6]). The most surprising effect of Zn^{2+} on the activity of β-barrel RNase **1** was observed in denaturation kinetics. Namely, the presence of Zn^{2+} delayed the reduction of β-barrel RNase **1** activity with increasing denaturant concentrations substantially (Figure 6, ■ vs ●). An increase from $\Delta G^{H_2O} = -1.2$ kcal/mol for metal-free to $\Delta G^{H_2O} = -2.9$ kcal/mol for "metallo-β-barrel" complexes in denaturant-free water was estimated by conventional data treatment.[23] Although, as already state above, any interpretation of these values needs much caution, it was at least qualitatively evident that Zn^{2+} stabilizes the "active" complex formed between β-barrel RNase **1** and RNA **2**. This finding was thus not only indicative for direct coordination of Zn^{2+} to histidine residues within β-barrel **1**, it provided, together with the already stabilizing effect of RNA alone on β-barrel **1** (Figure 6, ● vs ○), an additional illustration for the dynamic adaptability of rigid-rod β-barrels toward stabilization by templates.[17]

Product Analysis. β-Barrel phosphatase **1** could, *in principle*, cleave 18 different P−O bonds in 6-FAM-rU$_8$-6-TAMRA **2**. All phosphate diesters without vicinal hydroxy group are, of course, less likely candidates. However, a β-barrel RNase **1** could still produce either a random mixture of RNA fragments of different length, monomeric nucleotides, or selected oligomers only. The product mixture of β-barrel RNase **1** catalyzed hydrolysis of RNA **2** was separated by ion-exchange (IE) HPLC. Simplification of the IE-HPLC profile and sufficiently sensitive detection was achieved using a fluorescence detector that selectively monitored the intense emission of "6-TAMRA-free" 6-FAM-rU$_{0-8}$. It was possible to separate up to eight different 5′-labeled fragments using the mobile phase system reported by Stern and coworkers with minor modifications (Figure 8).[24] Control experiments with excess RNase A indicated that the base peak 1 represents the shortest possible fragment (Figure 8a), presumably a 6-FAM-rU$_1$, and that substrate 6-FAM-rU$_8$-6-TAMRA **2** is as poorly detectable under these conditions as expected from the presence of 6-TAMRA.

The regular pattern of the longer 6-FAM-rU$_{2-8}$ products eluting after the base peak demonstrated cleavability of several, if not all scissile P−O bonds by β-barrel RNase **1** (Figure 8c,d). Identical peaks obtained in control experiments for autohydrolysis and imidazole

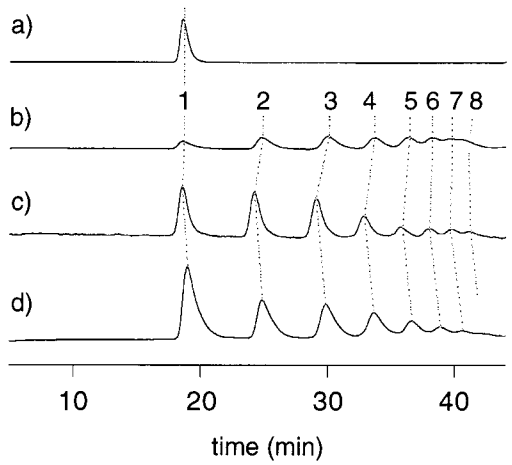

Figure 8. Typical ion-exchange HPLC profiles for 6-FAM-rU_{0-8} products obtained by hydrolysis of 200 nM 6-FAM-rU_8-6-TAMRA **2** with (a) excess RNase A, (b) autohydrolysis during ≥30 days, and 500 nM β-barrel **1** in (c) 17 h and (d) 18 days. Conditions: 50 mM HEPES, 50 °C, pH 7.0.

buffer-catalyzed hydrolysis of RNA **2** were in support of this interpretation (Figure 8b). We further noted that the shorter 5′-fragments (peaks 2, 3, and in part 4, Figure 8c) seem to be less suitable substrates for β-barrel RNase **1** than the longer 5′-oligomers (peaks 5−8, Figure 8c). This asymmetric product distribution (Figure 8c) was in contrast to that observed for autohydrolysis (Figure 8b) and other artificial RNases.[7a] It was maintained for 1 week of hydrolysis (Figure 8d). Although other explanations cannot be excluded, these observations can be considered as a first step toward more detailed studies on selectivity of oligonucleotide hydrolysis by multivalent rigid-rod β-barrel hydrolases with respect to oligomer length.

Summary and Perspectives

The objective of this study was to explore the usefulness of the first catalytic *p*-octiphenyl β-barrel for RNA cleavage. Using a doubly labeled uridine octamer as model substrate, a practical protocol to study the characteristics of RNase activity at relevant nanomolar concentrations was elaborated on the basis of previous reports in the literature. It was found that histidine-rich *p*-octiphenyl β-barrels accelerate the hydrolysis of this model substrate 32 000 times compared to imidazole in neutral water at nanomolar concentrations and 50 °C. Substrate binding and stabilization of the supramolecular barrel−substrate complex by the RNA template were observable by fluorescence resonance energy transfer and denaturation kinetics, respectively. Further rate enhancements were seen under mildly acidic conditions; modest rate enhancements accompanied by more substantial barrel−RNA complex stabilization in the presence of Zn^{2+} were noted as well as a likely preference for longer oligomer substrates.

These insights are encouraging for ongoing studies on *p*-octiphenyl β-barrel RNases on both the functional (e.g., scope and selectivity with respect to primary, secondary, and tertiary substrate structure) and the structural level (e.g., atomic force microscopy)[21a] as well as design and synthesis of novel *p*-octiphenyl β-barrels with refined properties.

This study focused on function rather than on structure. Whereas insights from several different lines of evidence[21a−c] provide overall satisfactory support for the *p*-octiphenyl β-barrel tertiary structure of substrate-free catalyst **1** (Figure 1), the suprastructure of the RNA−catalyst complex remains uncharacterized. Although binding of oligonucleotide duplexes within *p*-octiphenyl β-barrel ion channels (comprising internal lysines instead of histidines) has been demonstrated,[17d] it is thus not possible to judge whether RNA cleavage by artifical β-barrel **1** involves inclusion complex formation. Future structural studies will clarify eventual similarities with toroidal biomacromolecules such as the β-subunit of *E. coli* polymerase III[29a] and λ-exonuclease[29b] proposed early on[30] to be crucial for processive oligomer synthesis and degradation by substrate entrapment[29] and indicate eventual applicability of rigid-rod β-barrels in these directions. Ongoing efforts by several groups[31] to delineate the usefulness of biotechnologically modified ion channel sensors for oligonucleotide sequencing indicate that combination RNase and ion channel activity[21b] of rigid-rod β-barrels may lead to interesting applications as well.

Acknowledgment. We thank the Swiss NSF (21-57059.99 and National Research Program "Supramolecular Functional Materials" 4047-057496) for financial support.

References and Notes

(1) (a) Oivanen, M.; Kuusela, S.; Lönnberg, H. *Chem. Rev.* **1998**, *98*, 961. (b) Raines, R. T. *Chem. Rev.* **1998**, *98*, 1045. (c) Trawick, B. N.; Daniher, A. T.; Bashkin, J. K. *Chem. Rev.* **1998**, *98*, 939 and references therein and other reviews in this special issue of *Chem. Rev.*

(2) Molenveld, P.; Engbersen, J. F. J.; Reinhouldt, D. N. *Chem. Soc. Rev.* **2000**, *29*, 75.

(3) Häner, R. *Chimia* **2001**, *55*, 286.

(4) Perreault, D. M.; Anslyn, E. V. *Angew. Chem., Int. Ed. Engl.* **1997**, *36*, 432.

(5) Breslow, R. *Acc. Chem. Res.* **1991**, *24*, 317.

(6) (a) Breslow, R.; Huang, D.-L.; Anslyn, E. *Proc. Natl. Acad. Sci. U.S.A.* **1989**, *86*, 1746. (b) Breslow, R.; Labelle, M. *J. Am. Chem. Soc.* **1986**, *108*, 2655. (c) Breslow, R.; Berger, D.; Huang, D.-L. *J. Am. Chem. Soc.* **1990**, *112*, 3686.

(7) (a) Barbier, B.; Brack, A. *J. Am. Chem. Soc.* **1992**, *114*, 3511. (b) Barbier, B.; Brack, A. *J. Am. Chem. Soc.* **1988**, *110*, 6880.

(8) (a) Breslow, R.; Huang, D.-L. *Proc. Natl. Acad. Sci. U.S.A.* **1991**, *88*, 4080. (b) Anslyn, E.; Breslow, R. *J. Am. Chem. Soc.* **1989**, *111*, 8931. (c) Anslyn, E.; Breslow, R. *J. Am. Chem. Soc.* **1989**, *111*, 5972.

(9) (a) Giegé, R.; Felden, B.; Zenkova, A.; Silnikov, V. N.; Vlassov, V. V. *Methods Enzymol.* **2000**, *318*, 147. (b) Podyminogyn, M. A.; Vlassov, V. V.; Giegé, R. *Nucleic Acids Res.* **1993**, *21*, 5950.

(10) Konewetz, D. A.; Beck, I. E.; Beloglazova, N. G.; Sulimenkov, I. V.; Silnikov, V. N.; Zenkova, A.; Shishkin, G. V.; Vlassov, V. V. *Tetrahedron* **1999**, *55*, 503.

(11) (a) Vlassov, V. V.; Zuber, G.; Felden, B.; Behr, J.-P.; Giegé, R. *Nucleic Acids Res.* **1995**, *23*, 3161. (b) Guilley, H.; Jonard, G.; Kukla, B.; Richards, K. E. *Nucleic Acids Res.* **1979**, *6*, 1287.

(12) Helm, M.; Kopka, M. L.; Sharma, S. K.; Lown, J. W.; Giegé, R. *Biochem. Biophys. Res. Commun.* **2001**, *281*, 1283.

(13) Tung, C.-H.; Wei, Z.; Leibowitz, M. J.; Stein, S. *Proc. Natl. Acad. Sci. U.S.A.* **1992**, *89*, 7114.

(14) Lorente, A.; Espinosa, J. F.; Fernandez-Saiz, M.; Lehn, J.-M.; Wilson, W. D.; Zhong, Y. Y. *Tetrahedron Lett.* **1996**, *37*, 4417.

(15) (a) Beloglazova, N. G.; Silnikov, V. N.; Zenkova, A.; Vlassov, V. V. *FEBS Lett.* **2000**, *481*, 277. (b) Vlassov, V. V.; Abramova, T.; Godovikova, T.; Giegé, R.; Silnikov, V. N. *Antisense Nucleic Acid Drug Dev.* **1997**, *7*, 39.

(16) Reynolds, M. A.; Beck, T. A.; Say, P. B.; Schwartz, D. A.; Dwyer, B. P.; Daily, W. J.; Vaghefi, M. M.; Metzler, M. D.; Klem, R. E.; Arnold, L. J., Jr. *Nucleic Acids Res.* **1996**, *24*, 760.

(17) For rigid-rod β-barrels, please see: (a) Matile, S. *Chem. Rec.* **2001**, *1*, 162. (b) Das, G.; Sakai, N.; Matile, S. *Chirality* **2002**,

4, 18. (c) Das, G.; Matile, S. *Chirality* **2001**, *13*, 170. (d) Sakai, N.; Baumeister, B.; Matile, S. *ChemBioChem* **2000**, *1*, 123. (e) Baumeister, B.; Sakai, N.; Matile, S. *Angew. Chem., Int. Ed.* **2000**, *39*, 1955. (f) Baumeister, B.; Matile, S. *Chem. Eur. J.* **2000**, *6*, 1739. (g) Baumeister, B.; Matile, S. *Chem. Commun.* **2000**, 913. (h) Sakai, N.; Majumdar, N.; Matile, S. *J. Am. Chem. Soc.* **1999**, *121*, 4294.

(18) For introductions to β-barrels, please see: (a) Matile, S. *Chem. Soc. Rev.* **2001**, *30*, 158. (b) Stevenson, J. D.; Lutz, S.; Benkovic, S. J. *Angew. Chem., Int. Ed.* **2001**, *40*, 1854. (c) Gerlt, J. A. *Nat. Struct. Biol.* **2000**, ***7***, 171. (e) Nagano, N.; Hutchinson, E. G.; Thornton, J. M. *Protein Sci.* **1999**, *8*, 2072. (f) Buchanan, S. K. *Curr. Opin. Struct. Biol.* **1999**, *9*, 445. (g) Pujadas, G.; Palau, J. *Biologia (Bratislava)* **1999**, *54*, 231. (h) Flower, D. R. *Biochem. J.* **1996**, *318*, 1. (i) Hecht, M. H. *Proc. Natl. Acad. Sci. U.S.A.* **1994**, *91*, 8729.

(19) For introductions to rigid-rod molecules, please see: (a) Levin, M. D.; Kaszynski, P.; Michl, J. *Chem. Rev.* **2000**, *100*, 169. (b) Schwab, P. F. H.; Levin, M. D.; Michl, J. *Chem. Rev.* **1999**, *99*, 1863. (c) Berresheim, A. J.; Müller, M.; Müllen, K. *Chem. Rev.* **1999**, *99*, 1747. (d) Martin, R. E.; Diedrich, F. *Angew. Chem., Int. Ed.* **1999**, *38*, 1351.

(20) For similar use of *p*-oligoaryl rods, please see: (a) Fuji, K.; Furuta, T.; Tanaka, K. *Org. Lett.* **2001**, *3*, 169, 961. (b) Orner, B. P.; Ernst, J. T.; Hamilton, A. D. *J. Am. Chem. Soc.* **2001**, *123*, 5382. (c) Sakai, N.; Gerard, D.; Matile, S. *J. Am. Chem. Soc.* **2001**, *123*, 2517. (d) Read, M. W.; Escobedo, J.; Willis, D. M.; Beck, P. A.; Strongin, R. M. *Org. Lett.* **2000**, *2*, 3201. (e) Sakai, N.; Matile, S. *Chem. Eur. J.* **2000**, *6*, 1731. (f) Baxter, P. N. W.; Lehn, J.-M.; Baum, G.; Fenske, D. *Chem. Eur. J.* **1999**, *5*, 102. (g) Tanaka, K.; Furuta, T.; Fuji, K.; Miwa, Y.; Taga, T. *Tetrahedron Lett.* **1999**, *7*, 3001. (h) Winum, J.-Y.; Matile, S. *J. Am. Chem. Soc.* **1999**, *121*, 7961. (i) Tedesco, M. M.; Ghebremariam, B.; Sakai, N.; Matile, S. *Angew. Chem., Int. Ed.* **1999**, *38*, 540. (j) Lewis, P. T.; Strongin, R. M. *J. Org. Chem.* **1998**, *63*, 6065.

(21) For fibrillogenic activity of **1**, please see: (a) Das, G.; Ouali, L.; Adrian, M.; Baumeister, B.; Wilkinson, K. J.; Matile, S. *Angew. Chem., Int. Ed.* **2001**, *40*, 4657. For ion channel activity, esterase activity, and synthesis of **1**, please see: (b) Baumeister, B.; Sakai, N.; Matile, S. *Org. Lett.* **2001**, *3*, 4229. (c) Baumeister, B.; Som, A.; Sakai, N.; Vilbois, F.; Gerard, D.; Das, G.; Matile, S., Manuscript in preparation.

(22) Kelemen, B. R.; Klink, T. A.; Behlke, M. A.; Eubanks, S. R.; Leland, P. A.; Raines, R. T. *Nucleic Acids Res.* **1999**, *27*, 2696.

(23) Ahmad, F.; Bigelow, C. C. *J. Biol. Chem.* **1982**, *257*, 12935.

(24) Modak, A. S.; Gard, J. K.; Merriman, M. C.; Winkeler, K. A.; Bashkin, J. K.; Stern, M. K. *J. Am. Chem. Soc.* **1991**, *113*, 283.

(25) Haugland, R. P. *Handbook of Fluorescent Probes and Research Chemicals*, 6th ed.; Molecular Probes: Eugene, OR, 1996.

(26) Weiss, L. A.; Sakai, N.; Ghebremariam, B.; Ni, C.; Matile, S. *J. Am. Chem. Soc.* **1997**, *119*, 12142.

(27) (a) Saenger, W. *Principles of Nucleic Acid Structure*; Springer: New York, 1984. Examples: (b) Yoshinari, K.; Yamazaki, K.; Komiyama, M. *J. Am. Chem. Soc.* **1991**, *113*, 5899. (c) Akeson, M.; Branton, D. Kasianowicz, J. J.; Brandin, E.; Deamer, D. W. *Biophys. J.* **1999**, *77*, 3227.

(28) Mammen, M.; Choi, S.-K.; Whitesides, G. M. *Angew. Chem., Int. Ed.* **1998**, *37*, 2754.

(29) Oligonucleotides: (a) Kovall, R.; Mattews, B. W. *Science* **1997**, *277*, 1824. (b) Krishna, T. S.; Kong, X. P.; Gary, S.; Burgers, P. M.; Kuriyan, J. *Cell* **1994**, *79*, 1233. (c) Baker, T. A.; Bell, S. P. *Cell* **1998**, *92*, 295. Proteins: (d) Baumeister, W.; Walz, J.; Zühl, F.; Seemüller, E. *Cell* **1998**, *92*, 367. (e) Löwe, J.; Stock, D.; Jap, B.; Zwickl, P.; Baumeister, W.; Huber, R. *Science* **1995**, *268*, 534. (f) Joshua-Tor, L.; Xu, H. E.; Johnston, S. A.; Rees, D. C. *Science* **1995**, *269*, 945. Polyethylenes: (g) Kageyama, K.; Tamazawa, J.; Aida, T. *Science* **1999**, *285*, 2113.

(30) Klee, C. B.; Singer, M. F. *J. Biol. Chem.* **1968**, *243*, 923.

(31) (a) Howorka, S.; Cheley, S.; Bayley, H. *Nat. Biotechnol.* **2001**, *19*, 636. (b) Vercoutere, W.; Winters-Hilt, S.; Olsen, H.; Deamer, D.; Haussler, D.; Akeson, M. *Nat. Biotechnol.* **2001**, *19*, 248. (c) de Gennes, P.-G. *Proc. Natl. Acad. Sci. U.S.A.* **1999**, *96*, 7262. (d) Kasianowicz, J. J.; Brandin, E.; Branton, D.; Deamer, D. W. *Proc. Natl. Acad. Sci. U.S.A.* **1996**, *93*, 13770.

MA011612M